

Extracellular leucine-rich repeats as a platform for receptor/coreceptor complex formation

Yvon Jaillais^{a,b,1}, Youssef Belkhadir^{a,b,1,2}, Emilia Balsemão-Pires^{a,3}, Jeffery L. Dangl^{c,d,e}, and Joanne Chory^{a,b,4}

^aPlant Biology Laboratory, ^bThe Howard Hughes Medical Institute, Salk Institute for Biological Studies, La Jolla, CA 92037; and Departments of ^cBiology and ^dMicrobiology and Immunology, and ^eCurriculum in Genetics, Carolina Center for Genome Sciences, University of North Carolina, Chapel Hill, NC 27599

Contributed by Joanne Chory, March 4, 2011 (sent for review February 21, 2011)

Receptor kinases with leucine-rich repeat (LRR) extracellular domains form the largest family of receptors in plants. In the few cases for which there is mechanistic information, ligand binding in the extracellular domain often triggers the recruitment of a LRR-coreceptor kinase. The current model proposes that this recruitment is mediated by their respective kinase domains. Here, we show that the extracellular LRR domain of BRI1-ASSOCIATED KINASE1 (BAK1), a coreceptor involved in the disparate processes of cell surface steroid signaling and immunity in plants, is critical for its association with specific ligand-binding LRR-containing receptors. The LRRs of BAK1 thus serve as a platform for the molecular assembly of signal-competent receptors. We propose that this mechanism represents a paradigm for LRR receptor activation in plants.

brassinosteroid signaling | flagellin signaling | plant innate immunity | Receptor-like kinase | signaling crosstalk

Leucine-rich repeat receptor kinases (LRR-RKs) form the largest family of receptors in plants (1). LRR-RKs bind a wide range of ligands, including small molecule hormones and peptides, and are involved in a variety of developmental and immune signaling processes (2, 3). In *Arabidopsis*, BAK1 (BRI1-ASSOCIATED KINASE1) is an LRR coreceptor kinase for several LRR-RKs, including the brassinosteroid (BR) receptor BRI1 (BRASSINOSTEROID-INSENSITIVE 1) and the flagellin receptor FLS2 (FLAGELLIN-SENSING 2) that are involved in growth and immune responses, respectively (3–5). Ligand perception at the cell surface by either BRI1 or FLS2 induces the subsequent recruitment of BAK1 to a ligand-bound receptor complex (6–10). This process triggers transphosphorylation at multiple serines and threonines of the respective kinase domains inside the cell (11–13). Perhaps because BRI1 is a long-lived protein that apparently cycles between the plasma membrane and endosomes (14), there are multiple mechanisms to maintain the kinase domain in a basal state. BRI1 kinase is auto-inhibited by its C-terminal tail (15), by auto-phosphorylation on threonine 872 (11), and by a protein, BRI1 KINASE INHIBITOR 1 (BKI1), which associates with BRI1's kinase domain (10, 16). BKI1 inhibits BR signaling by binding to the BRI1's kinase domain, thereby inhibiting the interaction between BRI1- and BAK1-kinase (10, 16). Upon ligand binding, BRI1 phosphorylates BKI1 on a tyrosine within its membrane-targeting region, which dissociates BKI1 from the cell membrane and targets it to the cytoplasm, where it is inactive (10). Dissociation of BKI1 from BRI1 allows formation of a stable BRI1-BAK1 complex that is competent to induce downstream signaling (17).

The interplay between BRI1 and BAK1 kinase domains is further regulated by BAK1 autophosphorylation on tyrosine 610 (tyr-610), which is required to stimulate BRI1 kinase activity in vitro and for proper BR signaling in vivo (18). Of note, BAK1 tyr-610 phosphorylation is not required for flagellin response and it is possible that tyr-610 phosphorylation might be involved in the proper interaction with its cognate receptors. However, tyr-610 mutations affect only BRI1 kinase activation but not its interaction with BRI1 intracellular domain (18). Therefore, a critical unanswered question is how ligand-bound LRR-RKs selectively recruit

BAK1. Here, we report that the LRR domain of BAK1 is required for its recruitment to a ligand-bound LRR-RK and allows the kinase domains to be in physical contact for subsequent reciprocal transphosphorylation. Furthermore, our data indicate that the extracellular domain (ECD) of BAK1 is critical for the high affinity formation of the correct receptor/coreceptor pair.

Results and Discussion

Gain-of-Function Phenotype of *bak1^{elg}* Allele in the Brassinosteroid Pathway. A previously described mutation in *BAK1*, *elg* (*elongated*), was originally identified as a suppressor of the gibberellin biosynthesis mutant, *ga4* (19). The *elg* mutation results in a substitution of an aspartic acid to an asparagine (D122N) in the third LRR of BAK1 (20) (Fig. 1A and Fig. S1). The *elg* mutant is also hypersensitive to exogenous BR treatment (20). We found that both *elg* and transgenic lines of a null *bak1* mutant (*bak1-3*) (9), expressing *bak1^{elg}* fused with mCITRINE, a monomeric yellow variant of GFP (*bak1^{elg}::CITRINE*), had slightly longer hypocotyls in the dark compared with control plants (Fig. 1B and Fig. S1). Cell elongation in etiolated seedlings is BRI1-dependent (4). Importantly, in the presence of brassinazole (BRZ), an inhibitor of BR biosynthesis, both *elg* and *bak1-3* transgenic plants expressing a *bak1^{elg}::CITRINE* fusion protein still displayed partially elongated hypocotyls compared with controls (Fig. 1B and Fig. S1). These phenotypes were not explained by differential protein accumulation (Fig. 1D). Moreover, when grown in the light, both *elg* and the *bak1^{elg}::CITRINE*-expressing *bak1-3* transgenic plants exhibited long twisted petioles and elongated leaf blades (Fig. 1C and Fig. S1), and a rosette phenotype reminiscent of plants either overexpressing BRI1 or treated exogenously with BR (21).

We asked whether *bak1^{elg}::CITRINE* growth promotion is BRI1-dependent. We introgressed both *bak1^{elg}::CITRINE* and a complementing *BAK1::CITRINE* transgene into a *bri1*-null mutant. Both *BAK1::CITRINE* and *bak1^{elg}::CITRINE* failed to induce hypocotyl and petiole elongation in *bri1* plants (Fig. 1B and C). Finally, we checked the phosphorylation status of the BRI1-EMS-SUPPRESSOR 1 (BES1) transcription factor in *BAK1::CITRINE* and *bak1^{elg}::CITRINE* expressing *bak1-3* transgenic plants (Fig. 1E). BES1 phosphorylation is a readout for BR activity, as phosphorylated BES1 (P-BES1) is a mark of low BR signaling and dephosphorylated BES1 is indicative of active BR signaling (22). We found that *bak1^{elg}::CITRINE* but not

Author contributions: Y.J., Y.B., and J.C. designed research; Y.J., Y.B., and E.B.-P. performed research; Y.J., Y.B., E.B.-P., J.L.D., and J.C. analyzed data; and Y.J., Y.B., J.L.D., and J.C. wrote the paper.

The authors declare no conflict of interest.

See Commentary on page 8073.

¹Y.J. and Y.B. contributed equally to this work.

²Present Address: Moroccan Foundation for Advanced Science, Innovation and Research, Biotechnology Development Center, Technopolis Rabatshore, Sala al Jadida, 11100 Morocco.

³Present Address: Laboratório de Genômica Funcional e Transdução de Sinal, Departamento de Genética, Universidade Federal do Rio de Janeiro, 21944-970, Rio de Janeiro, Brazil.

⁴To whom correspondence should be addressed: E-mail: chory@salk.edu.

This article contains supporting information online at www.pnas.org/lookup/suppl/doi:10.1073/pnas.1103556108/-DCSupplemental.

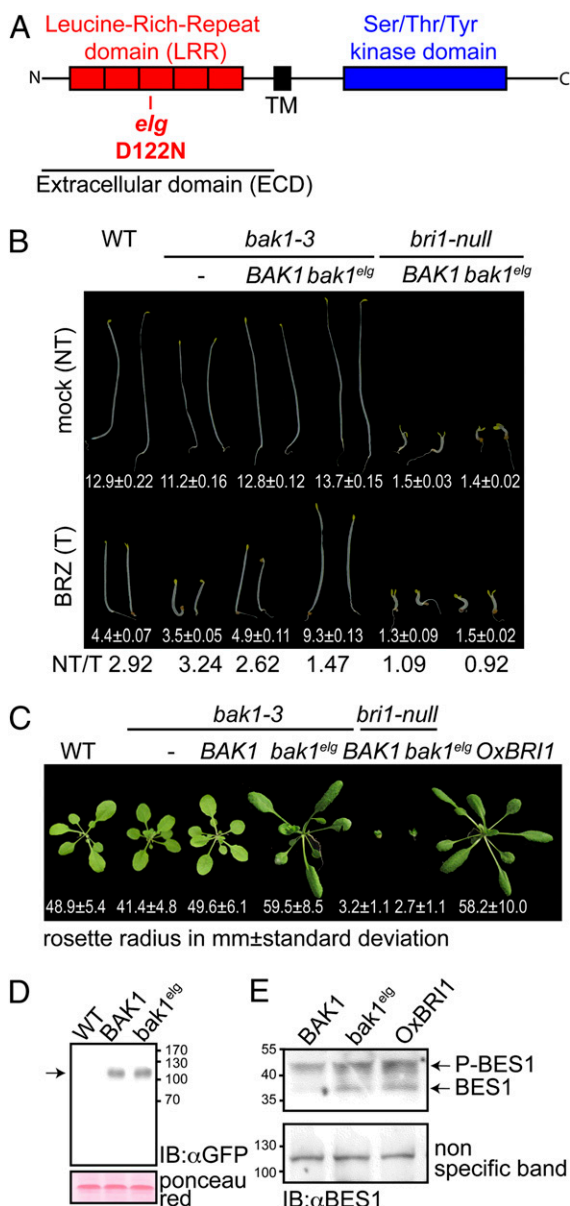


Fig. 1. Gain-of-function phenotype of *bak1^{elg}* allele for the brassinosteroid signaling pathway. (A) Schematic representation of BAK1 with its extracellular LRR domain in red and intracellular kinase domain in blue. TM: transmembrane segment. The position of the *elg* (D122N) mutation in BAK1 (LRR3) is indicated. (B) *BAK1prom::BAK1::CITRINE* expression complements the *bak1-3* hypocotyl growth defect. *BAK1prom::bak1^{elg}::CITRINE* expression in *bak1-3* leads to an elongated hypocotyl phenotype in the dark that is BRI1-dependent. Note that *BAK1prom::bak1^{elg}::CITRINE*-expressing hypocotyls still elongate when BR ligand is partially depleted by 1 μ M brassinazole, BRZ. Hypocotyl length is in mm \pm SD ($n = 25$), NT/T is the ratio of nontreated (NT) over BRZ-treated (T) hypocotyl length. (C) Pictures of rosette stage transgenic homozygous *Arabidopsis* (T3) expressing *BAK1prom::BAK1::CITRINE* or *BAK1prom::bak1^{elg}::CITRINE* under the control of the *BAK1* promoter in the *bak1-3* background. The phenotypes associated with the overexpression of BRI1 (on the right, for comparison), narrow leaf blades, elongated and twisting petioles were recapitulated by driving the expression of the *bak1^{elg}::CITRINE* variant. Mean value of rosette radius is indicated in mm \pm SD ($n = 25$). (D) BAK1::CITRINE accumulates to a similar extent as *bak1^{elg}::CITRINE*. Microsomal protein extracts were prepared from wild-type Col-0, *BAK1prom::BAK1::CITRINE* in *bak1-3* and *BAK1prom::bak1^{elg}::CITRINE* in *bak1-3* plants. These extracts were subjected to an anti-GFP protein immunoblot analysis to detect the accumulation of the CITRINE-tagged proteins. Equal loading was ensured by protein quantification before loading and by Ponceau red staining of the membrane postprotein transfer. (E) BES1

BAK1::CITRINE plants accumulated dephosphorylated BES1 to a similar extent as plants overexpressing BRI1. We conclude that *elg* acts as a gain-of-function mutation that requires BRI1 to promote cell elongation.

Impaired Flagellin Signaling of *bak1^{elg}*. To address the phenotype of *elg* and *bak1^{elg}::CITRINE* plants with respect to innate immune-response signaling, we monitored various readouts that include both early and late responses to flg22 (an elicitor peptide from bacterial flagellin) (3). Expression of BAK1::CITRINE, but not *bak1^{elg}::CITRINE*, in the *bak1-3* mutant almost completely rescued the induction of reactive oxygen species triggered by flg22, one of the earliest readouts for flagellin signaling (3) (Fig. 2A). Similarly, BAK1-CITRINE, but not *bak1^{elg}::CITRINE*, rescued the *bak1* phenotype with respect to loss of fresh weight and callose deposition triggered by flg22 late readouts of flagellin signaling (Fig. 2B and C). The *elg* mutant was also insensitive to flg22 treatments with respect to loss of fresh weight and callose deposition (Fig. S1D and E). Additionally, *bak1^{elg}::CITRINE bak1-3* plants did not exhibit protection from *Pseudomonas syringae* pv. *tomato* (Pto) DC3000 infection, which is normally induced in wild-type by cotreatment with flg22 (23) (Fig. 2D). Together, these results suggest that both early and late responses to flagellin are impaired by a single amino acid substitution in the ECD of BAK1. Importantly, *bak1^{elg}::CITRINE* selectively affected innate immune responses triggered by various MAMPs (microbe-associated molecular patterns) (Fig. S2). Together, our results indicate that the *bak1^{elg}* protein behaves differently with respect to BR signaling (gain-of-function) and flagellin responsiveness (loss-of-function).

D122N Substitution in BAK1's ECD Modifies its Interaction with Both BRI1 and FLS2 LRR-RKs. Next, we addressed the mechanism by which the *bak1^{elg}* protein induces BR signaling and blocks flagellin response. Control experiments showed that *bak1^{elg}::CITRINE* accumulates to similar levels as BAK1::CITRINE (Fig. 1D) and had a similar subcellular localization (Fig. S3A). In addition, the *elg* mutant had normal accumulation of BRI1 (Fig. S1), and expression of *bak1^{elg}::CITRINE* did not alter the accumulation of BRI1::CITRINE (Fig. 3A) or FLS2::GFP (Fig. 3B). Importantly, *bak1^{elg}::CITRINE* did not modify BRI1::mCITRINE or FLS2-GFP subcellular localization (Fig. S3B and C). Therefore, we hypothesized that the phenotypes ascribed to *bak1^{elg}* in Fig. 1 are the result of alterations in the interaction between *bak1^{elg}* and either BRI1 or FLS2.

Both BAK1::CHERRY and *bak1^{elg}::CHERRY* coimmunoprecipitated with BRI1::CITRINE in the absence of the brassinosteroid biosynthesis inhibitor, BRZ (Fig. 3A). In contrast, only *bak1^{elg}::CHERRY* coimmunoprecipitated with BRI1::CITRINE in the presence of BRZ (Fig. 3A). As described previously, flg22 treatment induced the recruitment of wild-type BAK1 to FLS2 (8, 9) (Fig. 3B). However, *bak1^{elg}::6xHA* did not coimmunoprecipitate with FLS2::GFP under these conditions (Fig. 3B). We could immunoprecipitate only a fraction of BAK1 with FLS2 after flg22 treatment; therefore, we cannot exclude the possibility that BAK1^{elg} can still bind to FLS2, albeit more weakly than wild-type BAK1. Taken together, our results indicate that the *bak1^{elg}* variant interacts with BRI1, even when the BR concentration is very low, whereas its ligand-induced interaction with FLS2 is impaired. These differences in affinity likely explain the opposite gain- and loss-of-function phenotypes in BR and flagellin signaling, respectively.

phosphorylation in *BAK1::CITRINE/bak1-3*, *BAK1-bak1^{elg}::CITRINE/bak1-3* and *OxBRI1* lines. P-BES is phosphorylated BES1. Equal loading was ensured by protein quantification before loading and by the signal intensity of a nonspecific band.

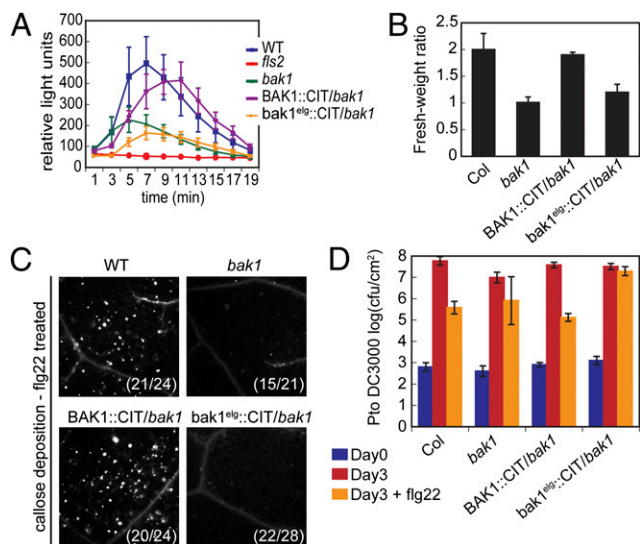


Fig. 2. *bak1^{elg}* has impaired flagellin response. (A) Oxidative burst triggered by 100 nM flg22 in wild-type Col-0 (blue), *fls2* (red), *bak1-3* (green), *BAK1prom:BAK1::CITRINE* in *bak1-3* (purple), *BAK1prom:bak1^{elg}::CITRINE* in *bak1-3* (orange) leaf discs measured in relative light units (RLU). Result are mean \pm SD ($n = 24$). (B) Average fresh-weight ratio of 14-d-old seedlings grown for 7 d in either water or water plus 1 μ M flg22. The bar graph represents the average fresh-weight ratio from wild-type Col-0, *bak1-3* mutant, *BAK1prom:BAK1::CITRINE* in *bak1-3*, and *BAK1prom:bak1^{elg}::CITRINE* in *bak1-3*. Means and SDs were calculated from 48 seedlings (six random pools of eight seedlings). (C) Callose deposits stained with aniline blue from leaves of wild type Col-0, *bak1-3*, *BAK1prom:BAK1::CITRINE* in *bak1-3* and *BAK1prom:bak1^{elg}::CITRINE* in *bak1-3* treated with 1 μ M flg22. The number of leaves showing the displayed features over the total in a given genotype is indicated in parentheses. (D) Growth of *Pseudomonas syringae* pv. *tomato* (Pto DC3000) was measured on the genetic backgrounds indicated at bottom. Leaves from 4-wk-old plants were infiltrated with a bacterial inoculum of 10^5 cfu mL⁻¹ in the presence (orange) or absence (red) of 1 μ M flg22 peptide. The number of bacteria per square centimeter of leaf was plotted on a log₁₀ scale. Error bars represent two times the SE among four internal replicate samples from one of three experiments.

BAK1 Kinase Activity Is Not Required for *bak1^{elg}* Association with BRI1. Previous reports indicated that the isolated kinase domains of BRI1 and BAK1 interact directly *in vitro* and in yeast (6, 7, 16, 18). It was therefore unexpected that the *bak1^{elg}* ECD mutation modified its interaction with both BRI1 and FLS2. One simple explanation for this could be that the LRRs of BAK1 interact directly with LRRs of BRI1 and *bak1^{elg}* enhances that interaction. Alternatively, *bak1^{elg}* may indirectly activate BAK1 kinase activity, thus enhancing the binding affinity between the two kinase domains. To explore these possibilities, we took advantage of the fact that strong overexpression of kinase-dead BAK1 leads to a dwarf phenotype because of impaired BR signaling (7). This phenotype is likely caused by a dominant-negative effect of the kinase-dead BAK1 on BRI1 kinase activity. In contrast, expression of a BAK1 kinase-dead mutant (D434N) under the control of its own promoter in wild-type plants did not induce a dwarf phenotype, probably because at this lower expression level, *bak1^{D434N}* is unable to compete with endogenous BAK1 to inhibit BRI1 activity (Fig. 4A). We reasoned that if *bak1^{elg}* activates its own kinase activity, then a double-mutant *bak1^{elg D434N}* would suppress any effect of the *elg* mutation. Alternatively, if the enhanced *bak1^{elg}* interaction with BRI1 is mediated by their respective ECDs, then *bak1^{elg D434N}* would bring the catalytically dead BAK1 kinase domain into proximity with the BRI1 kinase domain potentially enhancing any intrinsic dominant-negative effect on BRI1 activity, even at native *bak1^{elg D434N}* expression levels. In fact, we found that at similar expression levels, *bak1^{elg D434N}::CITRINE* but not

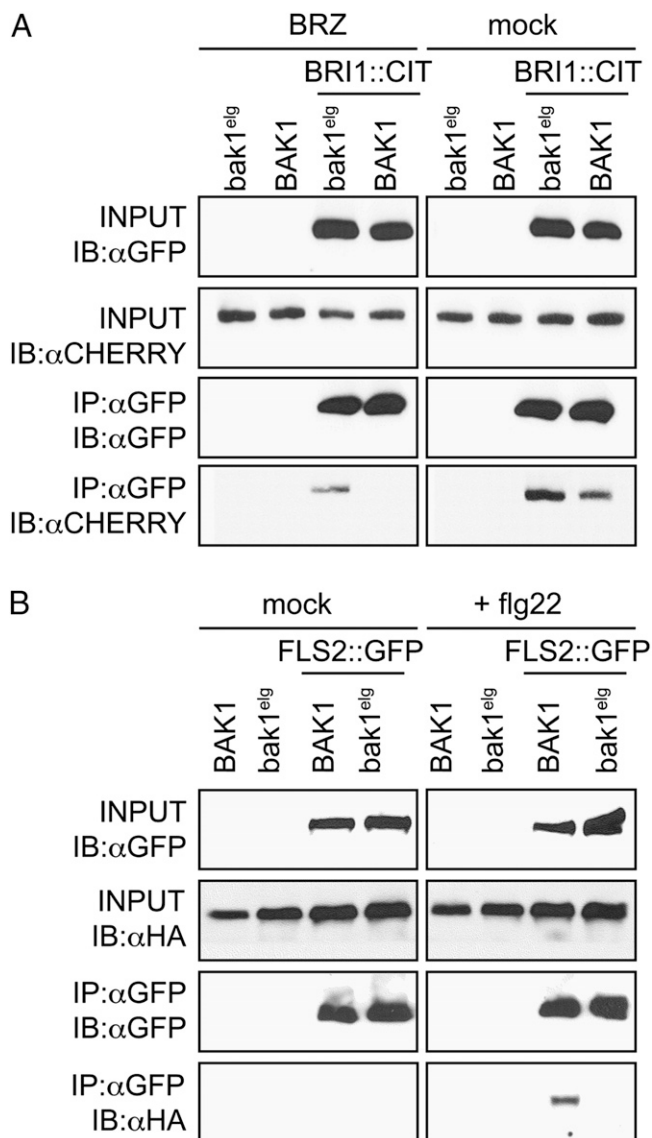


Fig. 3. A mutation in the extracellular LRR domain of BAK1 modifies its interaction with BRI1 and FLS2. (A) Transgenic *Arabidopsis* plants expressing either *BAK1prom:BAK1::CHERRY* or *BAK1prom:bak1^{elg}::CHERRY* alone or with *BRI1prom:BRI1::CITRINE* were grown with or without the BR biosynthesis inhibitor BRZ (5 μ M added from sowing of seeds). Total membrane protein was immunoprecipitated (IP) with anti-GFP antibodies and subjected to immunoblot (IB) analysis, as indicated. (B) Transgenic plants expressing either *BAK1prom:BAK1::6xHA* or *BAK1prom:bak1^{elg}::6xHA* alone or with *FLS2prom:FLS2::GFP* were grown on 1/2 LS media and treated 5 min before protein extraction with 10 μ M flg22. Total membrane protein was immunoprecipitated (IP) with anti-GFP antibodies and subjected to immunoblot (IB) analysis as indicated.

bak1^{D434N}::CITRINE resulted in a very strong dominant-negative phenotype; the plants were compact dwarfs that resembled mild to strong *bri1* mutants (Fig. 4A and B and Fig. S4). These results suggest that BAK1 is likely to interact with BRI1 through both its extracellular LRR domain, as well as its intracellular kinase domain, and that the *bak1^{elg}* mutation enhances this interaction.

BRI1 Receptor Complex Formation Involves a “Double-Lock” Mechanism. In conclusion, our study has identified a key role for the LRR ECD of the coreceptor BAK1 during recruitment to its receptors, BRI1 and FLS2. We propose a scenario in which LRR-containing coreceptors are recruited to their activated receptors

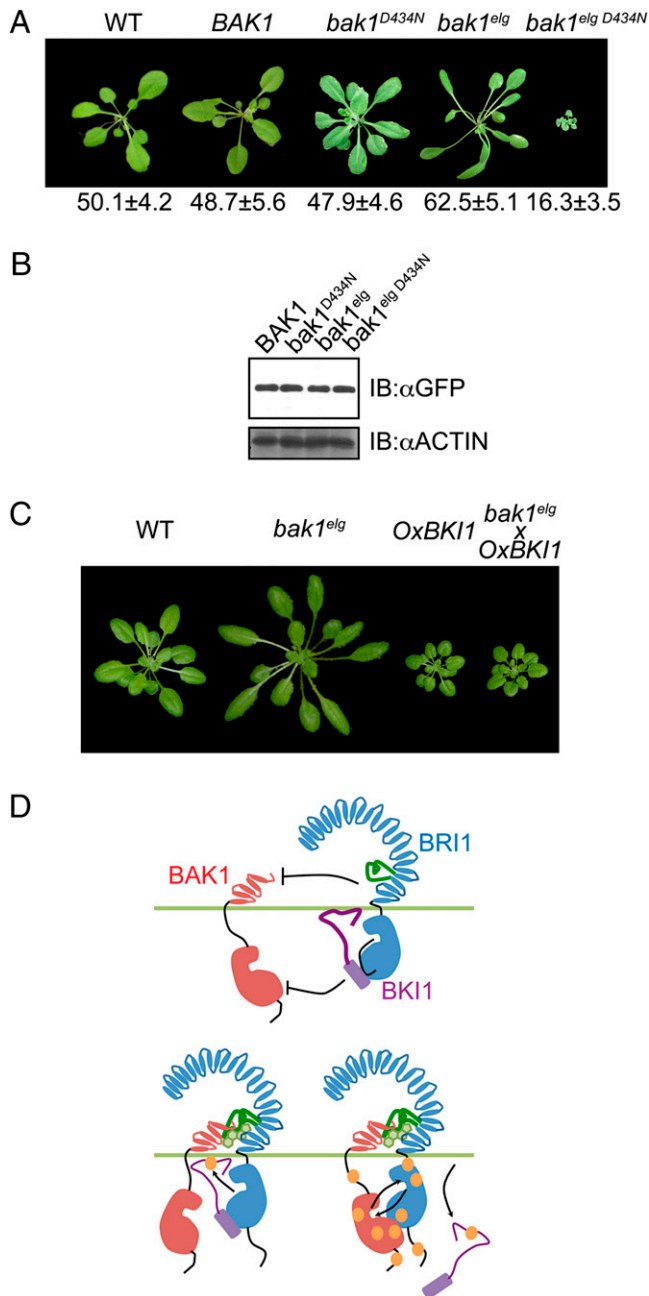


Fig. 4. BRI1 is activated by a double-lock mechanism. (A) Rosette leaf phenotype of wild-type Col-0, *BAK1prom::BAK1::CITRINE*, *BAK1prom::bak1^{D434N}::CITRINE*, *BAK1prom::bak1^{elg}::CITRINE*, and *BAK1prom::bak1^{elg D434N}::CITRINE*. Average rosette radius in mm ± SD ($n = 25$). (B) Expression level of transgenic proteins. (C) Rosette leaf phenotype of wild-type Col-0, *BAK1prom::bak1^{elg}::CITRINE*, *OxBKI1* and a cross between *BAK1prom::bak1^{elg}::CITRINE* and *OxBKI1* grown in short days. (D) Model for the formation of an active BR signaling complex. In the absence of ligand, BRI1 is maintained in an inactive state by its C-terminal tail as well as its inhibitory protein BKI1 and does not interact with BAK1 (Upper). Activation of BRI1 by BR triggers both the recruitment of BAK1 through its extracellular LRR domain as well as the BRI1-mediated phosphorylation of BKI1 inside the cell (Lower Left). This triggers dissociation of BKI1 from the plasma membrane and transphosphorylation between BRI1 and BAK1 kinase domain and leads to full activation of the receptor complex (Lower Right). BRI1 is represented as a monomer for simplicity but its isolated intracellular domain exist only as homodimers in solution (10) and 20% of the full-length receptor forms homodimers in vivo (30).

by their ECDs, bringing the receptor and coreceptor together and thus facilitating subsequent conformational changes and transphosphorylation of their kinase domains. Our finding that a single substitution in the third LRR of BAK1-ECD leads to a modification in its binding to both BRI1 and FLS2, with opposite phenotypic consequences, suggests that specific interactions between the ECDs are critical for the formation of the correct receptor/coreceptor pair. It is unlikely that *bak1^{elg}* hyperactivates the BR pathway by mass action because of its impaired interaction with FLS2. Indeed, BAK1 association with pattern recognition receptors is MAMP-dependent, but *bak1^{elg}* ectopically associates with BRI1 in the absence of MAMPs. As such, our data further suggest a fine-tuning between BR and MAMP signaling, where BAK1's affinity for the relevant receptors provides the cellular decision between elongation or defense. The third LRR of BAK1 plays a critical role in this decision as this region is involved in interaction with both BRI1 and FLS2.

The interaction between the activated BRI1 and BAK1 kinase domains is also critical, because a kinase-dead BRI1 does not interact with BAK1 in *planta* (12). Notably, we found that *bak1^{elg}* cannot reverse the phenotype induced by overexpression of BRI1 KINASE INHIBITOR1 (BKI1) (Fig. 4C), an inhibitory protein that prevents the interaction between BRI1 and BAK1 kinase domains (10). Therefore, we propose that receptor/coreceptor heterodimerization is regulated by a double-lock mechanism, in which both the ECDs and the kinase domains participate and which is a critical step for full receptor activation and downstream signaling (Fig. 4D). This strategy would provide room for multiple levels of regulation, coming both from outside and within the cell, in the form of noncell autonomous signals (e.g., ligand) and cell-autonomous regulators [e.g., inhibitory proteins like BKI1 (10)]. This double-lock mechanism would ensure both specificity and robustness in receptor complex formation and might represent a paradigm for LRR-RK activation. Of note, similar but not identical, strategies are used during activation of receptor tyrosine kinases (RTKs) in metazoans. Indeed, the ECDs of RTKs, such as the EGF receptor or the stem-cell factor receptor (KIT) homodimerize following ligand perception, which brings the kinases in the right orientation for *trans*-phosphorylation (24). In plants, the system is somewhat different in that receptor activation does not require ligand-induced homodimerization but heterodimerization with a coreceptor (3, 21). Because these coreceptors do not directly bind ligands, they are extremely labile and can be recruited to a variety of receptors. This invention allows one coreceptor, such as BAK1, to promote cell growth and innate immunity and, therefore, to be at a critical decision node as a plant determines to use resources to defend itself against microorganisms or to grow toward new resources [e.g., light, water, nutrients (25)]. Future challenges will be to understand the molecular basis of the recognition between receptor and coreceptor to better our understanding of signaling crosstalk.

Experimental Procedures

Plant Material and Growth Conditions. The wild-type used in all experiments was *A. thaliana* accession Columbia (Col-0) (except in Fig. S1, in which the wild-type control was accession Landsberg *erecta*, *Ler*). Plants were grown on either soil or Petri dishes containing 0.5× Linsmaier and Skoog medium (Caisson Laboratories) in long-day light conditions (16 h light/8 h dark). For bacterial assays, plants were grown in short-day conditions (8 h light/16 h dark). The mutants used in this study are the null *bak1-3* (9), the null *bri1* allele GABI_134E10, and the null *fls2* allele SALK_026801c. The insertion sites of the two T-DNA lines (GABI_134E10 and SALK_026801c) were located in the first exon of *BRI1* and *FLS2*, respectively. The homozygous mutations of *BRI1* and *FLS2* and the sequence of the insertion site were confirmed by PCR and sequencing. The *bri1* mutant was confirmed to be a null allele by Western blot using native anti-BRI1 polyclonal antibody against the C terminus of BRI1 (26). The functional *FLS2prom::FLS2::GFP* in the Col-0 background is a gift from Silke Robatzek (The Sainsbury Laboratory, Norwich, UK) (9).

Confocal Microscopy, Hormone, and Inhibitor Treatments. Microscopy and drug treatments were performed as described previously (27). Confocal microscopy was performed with a Leica SP2 inverted microscope and image analysis was done as described previously (28). BRZ (Chemiclones; 10 mM stock in DMSO) was used at the indicated concentration and was supplemented into the agar medium from the onset of germination.

Protein Extraction from Plants and Immunoprecipitation. Monoclonal anti-GFP HRP-coupled (Miltenyi Biotec), anti-HA-HRP coupled (Miltenyi Biotec), anti-ACTIN (clone C4; MP Biomedicals), and polyclonal anti-CHERRY (DsRed polyclonal; Clontech) were used at 1:5,000. Polyclonal anti-BRI1 [raised against BRI1 C terminus in rabbit] (26)] was used at 1:1,000. Flg22 treatment before protein extraction was done in liquid medium (0.5× Linsmaier and Skoog medium) for 5 min under vacuum. The immunoprecipitation extraction buffer was supplemented with 10 μ M flg22; the mock condition corresponds to addition of the same volume of water. Similarly, BRZ was supplied in the immunoprecipitation extraction buffer at a concentration of 5 μ M in the BRZ-treated condition; the mock condition corresponds to the addition of the same volume of DMSO (BRZ solvent). All immunoprecipitations were performed as previously described (28). Approximately 100 mg of 14-d-old light-grown seedlings were harvested for Western blot experiments. Immunoprecipitation experiments required from 1 to 3 g of seedlings (14-d-old). Tissues were ground at 4 °C in a 15-mL tube containing 2-mL of ice-cold sucrose buffer [20 mM Tris, pH 8; 0.33M Sucrose; 1 mM EDTA, pH 8; protease inhibitor (Roche)] using a polytron (Brinkman). Samples were centrifuged for 10 min at 5,000 \times g at 4 °C or until the supernatants were clear. This total protein fractions were centrifuged at 4 °C for 45 min at 20,000 \times g to pellet microsomes. The pellet was resuspended in 1 mL of immunoprecipitation buffer (50 mM Tris pH 8, 150 mM NaCl, 1% Triton X-100) using a 2-mL potter-Elvehjem homogenizer (Wheaton) and left on a rotating wheel for 30 min at 4 °C. Samples were then pelleted for 10 min at 20,000 \times g and 4 °C. The supernatant corresponded to the fraction enriched in microsomal associated proteins. The proteins were quantified and immunoprecipitates were performed on 1 mg of microsomal proteins. Each experiment was repeated at least three times and showed consistent results.

MAMP Response Assays. Flg22 (QRLSTGSRINSKDDAAGLQIA) and elf18 (acetyl-MSKEKFERTKPHVNVGTI) peptides were synthesized at >95% purity by ezbiolab and dissolved to a 10-mM stock in water. A pectidoglycan (Sigma-Aldrich) stock solution was prepared at 10 mg/mL in water. A 10 mg/mL chitin from shrimp shell (Sigma-Aldrich) stock solution was prepared as follows. Chitin powder was suspended in sterile PBS and sonicated at 25% output

power three times for 5 min with a sonicator. The suspension was then filtered with 100-, 70-, and 40- μ m sterile cell strainers. Following centrifugation (2,800 \times g, 10 min), chitin fragments from the 40- to 70- μ m fraction were suspended in the desired volume of sterile PBS and autoclaved. Oxidative burst assays were performed as described previously (9, 23), except that luminescence was measured using a Tecan Sapphire plate reader. Loss of fresh-weight ratio was calculated on 14-d-old seedlings grown for 7 d in either water or 1 μ M flg22 ($n = 48$, six random pools of eight seedlings). For callose deposition assays, 14-d-old plants were completely submerged in individual 0.5-mL Eppendorf tube containing the elicitor at the indicated concentration. A vacuum was applied for 15 min and plants remained in the elicitor solution for another 16 h. Next, seedlings were fixed in a 3:1 ethanol:acetic acid solution for several hours. Seedlings were rehydrated in 70% ethanol for 2 h, 50% ethanol for an additional 2 h, and then with water overnight. Seedlings were then incubated in 150 mM K_2HPO_4 , pH 9.5, and 0.01% Aniline blue (Sigma-Aldrich) for several hours. Individual leaves were mounted on slides in 50% glycerol, and callose was observed immediately using a Leica DM5000B under UV (excitation, 390 nm; emission, 460 nm). Bacterial assays were performed as described earlier (23, 29) except that bacterial count were assayed at 3 d postinfection. Each experiment was repeated at least three times and showed consistent results.

ACKNOWLEDGMENTS. We thank W. Chen and T. Dabi for technical assistance; M. Dreux, E. Kaiserli, U. Pedmale, G. Vert, and M. Hothorn, and M. Nishimura and P. Epple for providing critical feedback on the manuscript; The Max Planck Society and the Salk Institute for providing the insertion mutant lines; S. Robatzek for providing the *FLS2prom::FLS2::GFP* in Col-0; N. Geldner for providing pNIGEL; J. Long for providing pBJ36; R. Tsien for providing mCHERRY and mCITRINE fluorescent tags; Y. Yin for providing anti-BES1 antibody; and the Nottingham Arabidopsis Stock Centre and Arabidopsis Biological Resource Center for providing material. These studies were supported by the Howard Hughes Medical Institute and Grant IOS-0649389 from the National Science Foundation (to J.C.), and by Grants GM057171 and GM066025 from the National Institutes of Health and Grant IOS-0929410 from the National Science Foundation's Arabidopsis 2010 Program (to J.L.D.); and National Science Foundation Grant IOS-0649389 (to J.C.). Y.B. was a Howard Hughes Medical Institute fellow of the Life Sciences Research Foundation and also received support from the Philippe Foundation; Y.J. was supported by a fellowship from the European Molecular Biology Organization and in part by the Marc and Eva Stern Foundation; E.B-P was supported by a PhD fellowship from CAPES (Coordenação de Aperfeiçoamento de Pessoal de Nível Superior) and an SWE (SANDWICHE) fellowship from CNPq (Conselho Nacional de Desenvolvimento Científico e Tecnológico).

- Shiu SH, Bleecker AB (2001) Receptor-like kinases from *Arabidopsis* form a monophyletic gene family related to animal receptor kinases. *Proc Natl Acad Sci USA* 98:10763–10768.
- De Smet I, Voss U, Jürgens G, Beekman T (2009) Receptor-like kinases shape the plant. *Nat Cell Biol* 11:1166–1173.
- Boller T, Felix G (2009) A renaissance of elicitors: Perception of microbe-associated molecular patterns and danger signals by pattern-recognition receptors. *Annu Rev Plant Biol* 60:379–406.
- Vert G, Nemhauser JL, Geldner N, Hong F, Chory J (2005) Molecular mechanisms of steroid hormone signaling in plants. *Annu Rev Cell Dev Biol* 21:177–201.
- Gómez-Gómez L, Boller T (2000) FLS2: An LRR receptor-like kinase involved in the perception of the bacterial elicitor flagellin in *Arabidopsis*. *Mol Cell* 5:1003–1011.
- Nam KH, Li J (2002) BRI1/BAK1, a receptor kinase pair mediating brassinosteroid signaling. *Cell* 110:203–212.
- Li J, et al. (2002) BAK1, an Arabidopsis LRR receptor-like protein kinase, interacts with BRI1 and modulates brassinosteroid signaling. *Cell* 110:213–222.
- Heese A, et al. (2007) The receptor-like kinase SERK3/BAK1 is a central regulator of innate immunity in plants. *Proc Natl Acad Sci USA* 104:12217–12222.
- Chinchilla D, et al. (2007) A flagellin-induced complex of the receptor FLS2 and BAK1 initiates plant defence. *Nature* 448:497–500.
- Jaillais Y, et al. (2011) Tyrosine phosphorylation controls brassinosteroid receptor activation by triggering membrane release of its kinase inhibitor. *Genes Dev* 25:232–237.
- Wang X, et al. (2005) Identification and functional analysis of in vivo phosphorylation sites of the Arabidopsis BRASSINOSTEROID-INSENSITIVE1 receptor kinase. *Plant Cell* 17:1685–1703.
- Wang X, et al. (2008) Sequential transphosphorylation of the BRI1/BAK1 receptor kinase complex impacts early events in brassinosteroid signaling. *Dev Cell* 15:220–235.
- Schulze B, et al. (2010) Rapid heteromerization and phosphorylation of ligand plant transmembrane receptors and their associated kinase BAK1. *J Biol Chem* 285:9444–9451.
- Geldner N, Hyman DL, Wang X, Schumacher K, Chory J (2007) Endosomal signaling of plant steroid receptor kinase BRI1. *Genes Dev* 21:1598–1602.
- Wang X, et al. (2005) Autoregulation and homodimerization are involved in the activation of the plant steroid receptor BRI1. *Dev Cell* 8:855–865.
- Wang X, Chory J (2006) Brassinosteroids regulate dissociation of BK1, a negative regulator of BRI1 signaling, from the plasma membrane. *Science* 313:1118–1122.
- Kim T-W, et al. (2009) Brassinosteroid signal transduction from cell-surface receptor kinases to nuclear transcription factors. *Nat Cell Biol* 11:1254–1260.
- Oh M-H, et al. (2010) Autophosphorylation of Tyr-610 in the receptor kinase BAK1 plays a role in brassinosteroid signaling and basal defense gene expression. *Proc Natl Acad Sci USA* 107:17827–17832.
- Halliday K, Devlin PF, Whitelam GC, Hanhart C, Koornneef M (1996) The *ELONGATED* gene of *Arabidopsis* acts independently of light and gibberellins in the control of elongation growth. *Plant J* 9:305–312.
- Whippo CW, Hangarter RP (2005) A brassinosteroid-hypersensitive mutant of BAK1 indicates that a convergence of photomorphogenic and hormonal signaling modulates phototropism. *Plant Physiol* 139:448–457.
- Belkhadir Y, Chory J (2006) Brassinosteroid signaling: A paradigm for steroid hormone signaling from the cell surface. *Science* 314:1410–1411.
- Vert G, Chory J (2006) Downstream nuclear events in brassinosteroid signalling. *Nature* 441:96–100.
- Zipfel C, et al. (2004) Bacterial disease resistance in *Arabidopsis* through flagellin perception. *Nature* 428:764–767.
- Lemmon MA, Schlessinger J (2010) Cell signaling by receptor tyrosine kinases. *Cell* 141:1117–1134.
- Jaillais Y, Chory J (2010) Unraveling the paradoxes of plant hormone signaling integration. *Nat Struct Mol Biol* 17:642–645.
- Belkhadir Y, et al. (2010) Intragenic suppression of a trafficking-defective brassinosteroid receptor mutant in *Arabidopsis*. *Genetics* 185:1283–1296.
- Jaillais Y, Fobis-Loisy I, Miège C, Rollin C, Gaude T (2006) AtSNX1 defines an endosome for auxin-carrier trafficking in *Arabidopsis*. *Nature* 443:106–109.
- Jaillais Y, et al. (2007) The retromer protein VPS29 links cell polarity and organ initiation in plants. *Cell* 130:1057–1070.
- Zipfel C, et al. (2006) Perception of the bacterial PAMP EF-Tu by the receptor EFR restricts Agrobacterium-mediated transformation. *Cell* 125:749–760.
- Hink MA, Shah K, Russinova E, de Vries SC, Visser AJWG (2008) Fluorescence fluctuation analysis of *Arabidopsis thaliana* somatic embryogenesis receptor-like kinase and brassinosteroid insensitive 1 receptor oligomerization. *Biophys J* 94:1052–1062.

Supporting Information

Jaillais et al. 10.1073/pnas.1103556108

SI Experimental Procedures

Constructs, Generation of Transgenic Lines, and Phenotype Analysis.

The mCITRINE-tagged lines are resistant to glufosinate (Basta), 6xHA-tagged lines to kanamycin, and mCHERRY-tagged lines to hygromycin. Rosette radius phenotypes were quantified on 5-wk-old plants. *UBQ10prom* was PCR amplified from pNIGEL (1) (gift from N. Geldner, University of Lausanne), *35Sprom* from pBJ36 (gift from J. Long, Salk Institute, La Jolla, CA), *BRI1prom* (1.7 kb), *BAK1prom* (1.7 kb) from Col-0 genomic DNA, and cloned into *pDONR-P4P1R* using the gateway recombination system (Invitrogen) (see [Table S1](#) for primers). *BRI1*, *BAK1*, and *BKII* were PCR-amplified from Col-0 genomic DNA and recombined into *pDONR221* (Invitrogen). Monomeric *CHERRY* (2), monomeric *CITRINE* (3) (gifts from R. Tsien, University of California San Diego), and *6xHA* (pBJ36, gift from J. Long, Salk Institute) were cloned into *pDONR-*

P2RP3 (Invitrogen). Site-directed mutagenesis was carried out following the site-directed mutagenesis protocol from Agilent Technology (formerly Stratagene) using the primers listed in [Table S1](#). Final destination vectors were obtained by using a three-fragment recombination system using the *pB7m34GW*, *pH7m34GW*, and *pK734GW* destination vectors (4). The constructs created are listed in [Table S2](#). *BRI1* and *BAK1* constructs were transformed into heterozygous *bri1* (GABI_134E10) and homozygous *bak1-3*, respectively, and their transgenic expression fully rescued the *bri1*^{-/-} and *bak1*^{-/-} growth defects. For all constructs, more than 20 independent T1 lines were isolated and between three and eight representative monoinsertion lines were selected in the T2 generation. Confocal microscopy, phenotypic analysis and protein extraction were performed on segregating T2 and homozygous T3 lines.

1. Geldner N, et al. (2009) Rapid, combinatorial analysis of membrane compartments in intact plants with a multicolor marker set. *Plant J* 59:169–178.
2. Shaner NC, et al. (2004) Improved monomeric red, orange and yellow fluorescent proteins derived from *Discosoma* sp. red fluorescent protein. *Nat Biotechnol* 22: 1567–1572.

3. Griesbeck O, Baird GS, Campbell RE, Zacharias DA, Tsien RY (2001) Reducing the environmental sensitivity of yellow fluorescent protein. Mechanism and applications. *J Biol Chem* 276:29188–29194.
4. Karimi M, Bleys A, Vanderhaeghen R, Hilson P (2007) Building blocks for plant gene assembly. *Plant Physiol* 145:1183–1191.

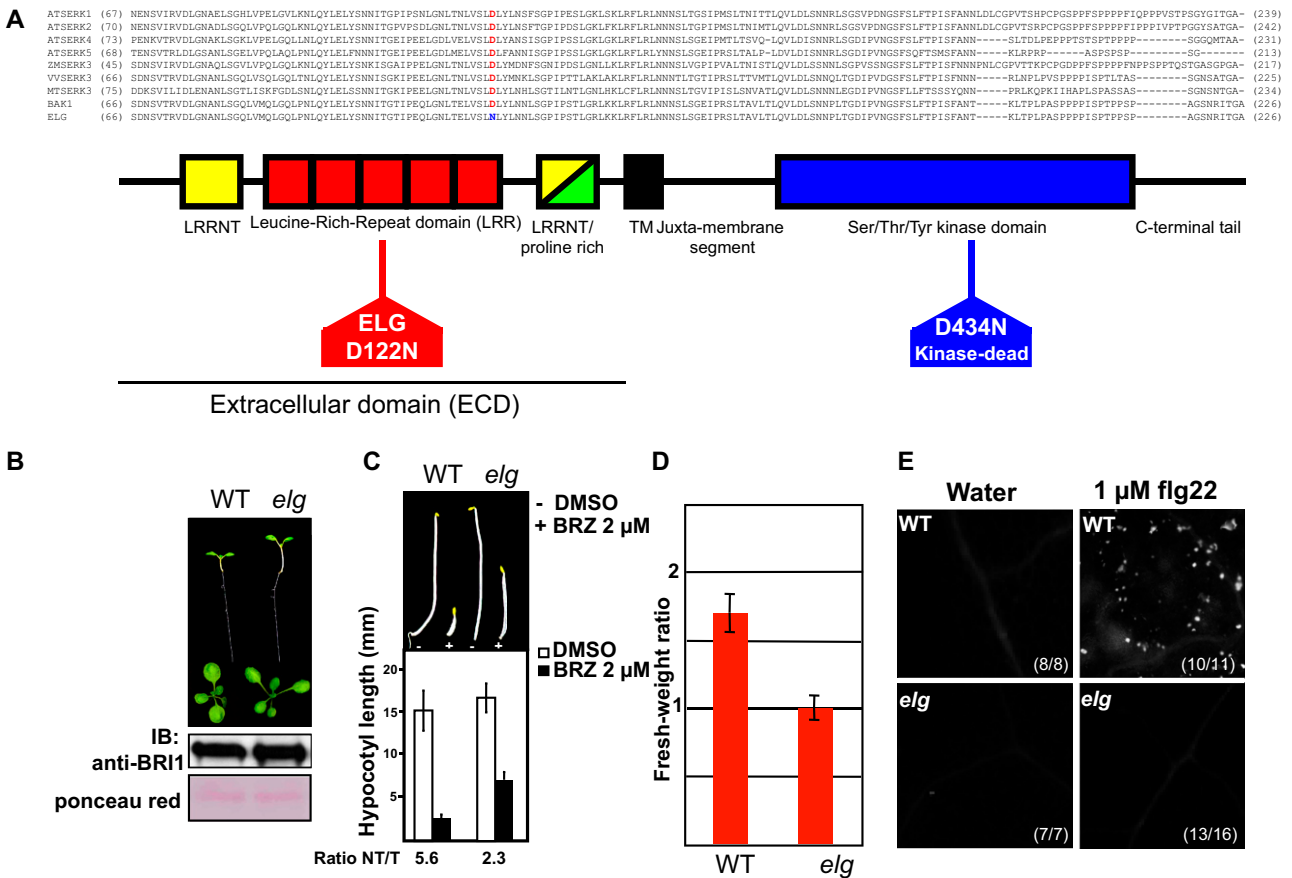


Fig. S1. Phenotype characterization of the *bak1* mutant allele *elongated*. The *elongated* (*elg*) mutant was initially identified as a suppressor of the GA biosynthetic mutant *ga4* by a forward genetic screen (1, 2). This mutant was shown to display a robust enhancement of high-light phototropism compared with wild-type plants but retained a normal very low light response (2). (A) *elg* was mapped to the extracellular domain of *BAK1*. *elg* is a D122N missense mutation in the extracellular leucine-rich receptor (LRR) domain of *BAK1* (2). (Upper) The alignment between the *Arabidopsis thaliana* *BAK1* (also known as *SERK3* for SOMATIC EMBRYOGENESIS RECEPTOR KINASE3) and its paralogs in *A. thaliana* (*AtSERK1* to *AtSERK5*) as well as its orthologs in various plant species. Note that D122 is conserved in all *BAK1* paralogs and orthologs, suggesting functional importance. (Lower) A schematic representation of *BAK1* architecture. LRRNT: LRR N-terminal domain, LRRCT: LRR C-terminal domain (note that this domain is present in *SERK1*, 2 and 5 but not in *BAK1/SERK3* and *SERK4*, where it is replaced by a proline-rich region), TM: transmembrane region. The sequence alignment was performed as follows: each sequence was run through the pfam program (<http://www.sanger.ac.uk>) to determine the position of the LRRNT and through the TMHMM program (<http://www.cbs.dtu.dk/services/TMHMM>) to determine the position of the transmembrane segment. The sequence between the LRRNT and the TM (LRR domain + LRRCT/proline-rich domain) were then aligned using tcoffee (<http://www.tcoffee.org>). The position of the point mutant used in this study are indicated: ELG = D122N (red) and we used the canonical Asp-to-Asn kinase-dead mutation (D434N; blue). We found that mutant protein to be more stable both in vivo and in vitro than the previously used K317E kinase dead mutation. *AtSERK1*, At1g71830; *AtSERK2*, At1g34830; *AtSERK3/BAK1*, At4g33430; *AtSERK4*, At2g13790; *AtSERK5*, At2g13800; *MtSERK3*, *Medicago truncatula* ADO15298.1; *VvSERK3*, *Vitis vinifera* CBI20070.3; *ZmSERK3* Zea mays CAC37642.1. (B) *elg* mutants display phenotypes consistent with plants treated with brassinosteroids or plants overexpressing *BRI1*. Representative pictures of 10-d-old seedlings (Top) and rosette stage (*Middle*) *Arabidopsis* plants grown under identical conditions are shown. The gain-of-function phenotypes of *elg* plants are not due to the overaccumulation of *BRI1*. Microsomal protein extracts prepared from accession *Ler* (*Landsberg erecta*) and isogenic *elg* plants were subjected to an anti-*BRI1* protein immunoblot analysis. Equal loading was ensured by protein quantification before loading and by Ponceau red staining of the membrane postprotein transfer. (C) *elg* dark-grown seedlings are resistant to brassinazole (BRZ), an inhibitor of BR biosynthesis. Morphology of 4-d-old dark-grown seedlings of wild-type *Ler* and *elg* grown on half-strength MS medium in the absence (–) or presence (+) of 2 μM brassinazole (BRZ) (Upper). Length of 4-d-old dark-grown seedlings in the absence (white bars) or presence (black bars) of 2 μM brassinazole (BRZ). Means and SDs were calculated from ~40 seedlings (Lower). The ratio of the average hypocotyl length of nontreated (NT) to treated (T) seedlings is indicated at the bottom. (D) Average fresh-weight ratio of 14-d-old seedlings grown for 7 d in either water or 1 μM flg22 (Left). The red bar represents the average fresh-weight ratio from wild-type *Ler* and isogenic *elg* seedlings. Means and SDs were calculated from ~48 seedlings (six random pools of eight seedlings). (E) Callose deposition was stained with aniline blue in the leaves of wild-type accession *Ler* and *elg* seedlings treated with water or 1 μM flg22 (Right). The fraction of leaf showing the displayed features is given in parenthesis. Because *elg* is in *Landsberg erecta* background and our reference accession is *Columbia-0*, we took a transgenic approach and expressed *BAK1* and *bak1^{elg}* (tagged with the monomeric fluorescent protein CITRINE) in a *bak1-3* mutant (*Col-0* background). The rest of the mutant phenotype characterization was carried out with those lines.

- Halliday K, Devlin PF, Whitelam GC, Hanhart C, Koornneef M (1996) The ELONGATED gene of *Arabidopsis* acts independently of light and gibberellins in the control of elongation growth. *Plant J* 9:305–312.
- Whippo CW, Hangarter RP (2005) A brassinosteroid-hypersensitive mutant of *BAK1* indicates that a convergence of photomorphogenic and hormonal signaling modulates phototropism. *Plant Physiol* 139:448–457.

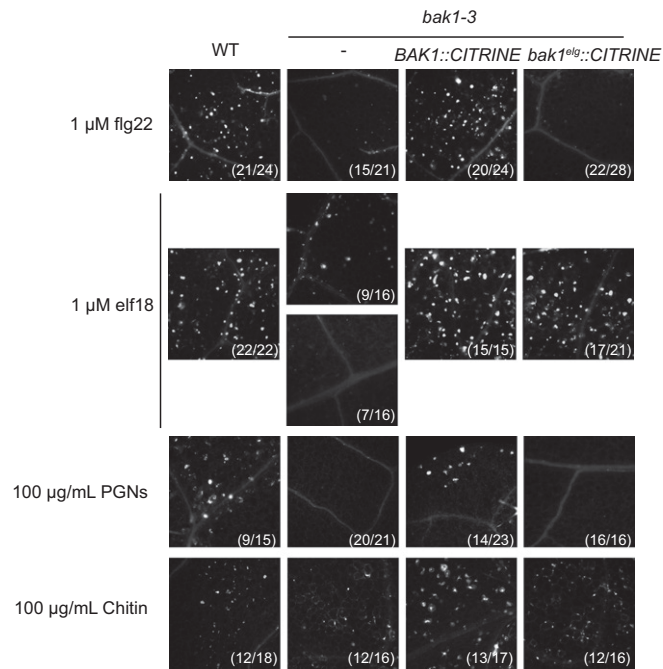


Fig. S2. *bak1^{elg}* selectively eliminates flg22- and peptidoglycan- (PGN) but not elf18-induced callose deposition. The first line of active defense relies on the recognition of microbe-associated molecular patterns (MAMPs) by pattern recognition receptors (PRRs) (1). Among these responses to MAMPs, some are BAK1-dependent and others are BAK1-independent. To test whether *bak1^{elg}* affects only flg22 response, all aspect of BAK1-dependent immunity or MAMP-triggered Immunity (MTI) in general, we tested several MAMPs known to be either BAK1-dependent or -independent. In *Brassicaceae*, a peptide corresponding to the *N*-acetylated N-terminal 18 amino acids of bacterial EF-Tu (elf18) is recognized by a receptor called EFR (for EF-Tu Receptor) and triggers MAMP-triggered Immunity (1). Like FLS2, EFR function is partially dependent on BAK1 (2). PGNs are a major cell-wall component of Gram-positive bacteria and are recognized as a MAMP in *Arabidopsis*. The receptor for PGNs is unknown but this response is BAK1-dependent (1). Finally, chitin, an important component of the cell wall of fungi, is also recognized as a MAMP in *Arabidopsis*. Interestingly, the plant chitin receptor RLK1/CERK1 is a LysM receptor-like Kinase and do not have LRR in its extracellular domain (3, 4). This finding is consistent with the observation that chitin response is BAK1-independent. Callose deposits were stained with aniline blue in the leaves of wild-type *Col-0*, *bak1-3*, *BAK1prom:BAK1::CITRINE* in *bak1-3*, *BAK1prom:bak1^{elg}::CITRINE* in *bak1-3* seedlings treated with 1 μM flg22, 1 μM elf18, 100 μg/mL of PGNs, or 100 μg/mL of chitin for 16 h. The fraction of leaf showing the displayed features is shown in parenthesis. Note that elf18-induced callose deposition was extremely robust in wild-type *Col-0* and was not completely abolished in about half of *bak1-3* plant analyzed. We saw this partial response when looking at well-emerged true leaves but not cotyledons. In contrast, PGNs and chitin-induced callose deposition was not observed in all of the wild-type *Col-0* leaves observed. Nevertheless, the PGN- but not chitin-induced callose deposition was clearly reduced in *bak1-3* and *BAK1prom:bak1^{elg}::CITRINE* in *bak1-3*. These results indicate that *bak1^{elg}* selectively affected innate immune responses triggered by various MAMPs, it behaves as a loss-of-function with respect to flg22/FLS2 and PNG responses, but it is neutral for elf18/EFR function.

1. Boller T, Felix G (2009) A renaissance of elicitors: Perception of microbe-associated molecular patterns and danger signals by pattern-recognition receptors. *Annu Rev Plant Biol* 60: 379–406.
2. Chinchilla D, et al. (2007) A flagellin-induced complex of the receptor FLS2 and BAK1 initiates plant defence. *Nature* 448:497–500.
3. Iizasa E, Mitsutomi M, Nagano Y (2010) Direct binding of a plant LysM receptor-like kinase, LysM RLK1/CERK1, to chitin in vitro. *J Biol Chem* 285:2996–3004.
4. Petutschnig EK, Jones AME, Serazetdinova L, Lipka U, Lipka V (2010) The lysin motif receptor-like kinase (LysM-RLK) CERK1 is a major chitin-binding protein in *Arabidopsis thaliana* and subject to chitin-induced phosphorylation. *J Biol Chem* 285:28902–28911.

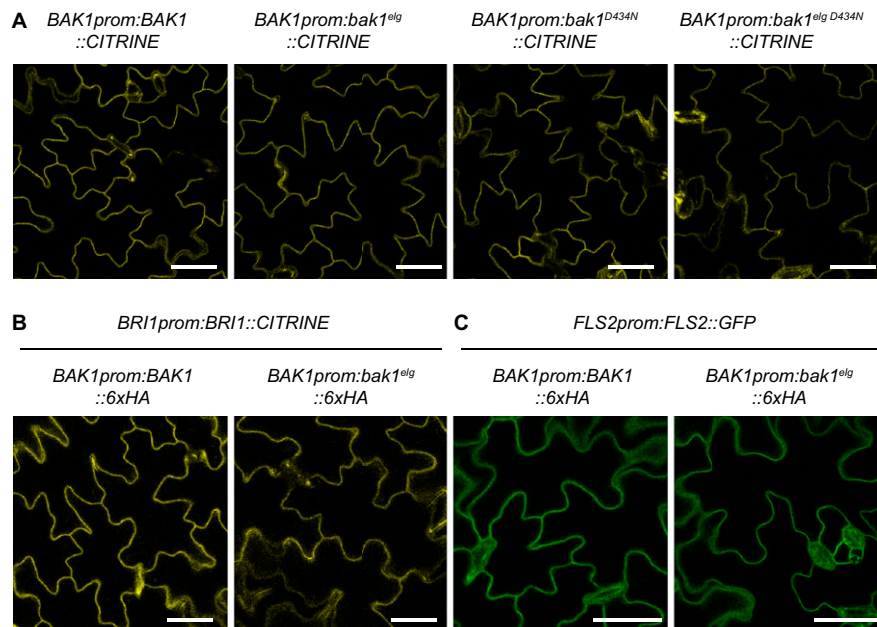


Fig. S3. Subcellular localization of the different BAK1 mutants and effect of $bak1^{elg}$ on BRI1/FLS2 subcellular localization. (A) Representative confocal pictures of the cotyledon of $BAK1prom:BAK1::CITRINE$, $BAK1prom:bak1^{elg}::CITRINE$, $BAK1prom:bak1^{D434N}::CITRINE$, and $BAK1prom:bak1^{elg D434N}::CITRINE$ T3 homozygous lines. Identical confocal settings were used for each of the picture shown. (B) Representative confocal pictures of cotyledon of $BRI1prom:BRI1::CITRINE$ in $BAK1prom:BAK1::6xHA$ and $BAK1prom:bak1^{elg}::6xHA$ expressing lines, respectively. The same confocal settings were used for both pictures. (C) Representative confocal pictures of cotyledon of $FLS2prom:FLS2::GFP$ in $BAK1prom:BAK1::6xHA$ and $BAK1prom:bak1^{elg}::6xHA$ expressing lines, respectively. The same confocal settings were used for both pictures. (Scale bars, 20 μm .)

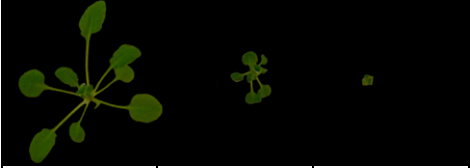
T1			
	Wild type	Dwarf	Severe dwarf
$BAK1prom:BAK1^{D434N}::CITRINE$	189	16	0
$BAK1prom:bak1^{elg D434N}::CITRINE$	116	61	24

Fig. S4. Quantification of T1 phenotype of $BAK1prom:bak1^{D424N}::CITRINE$ and $BAK1prom:bak1^{elg D434N}::CITRINE$. Because some $bak1^{elg D434N}::CITRINE$ expressing T1 plants had a very strong *bri1*-like phenotype and could not set seeds, and some $bak1^{D434N}::CITRINE$ T1 lines showed a mild phenotype, we decided to score the phenotype of individual T1 plants. We divided these phenotypes into three different categories: no obvious phenotypes (wild-type), dwarf, and severe dwarves (plants in the severe dwarf category had a phenotype similar to a strong *bri1* and could not set seeds). We found no $BAK1prom:bak1^{D434N}::CITRINE$ plant in the severe dwarf category; 12% of $BAK1prom:bak1^{elg D434N}::CITRINE$ T1 plants (24 out of 201) were ranked in that category. Furthermore, only 8% of $BAK1prom:bak1^{D434N}::CITRINE$ T1 plants (16 of 205) showed a dwarf phenotype against 30% of $BAK1prom:bak1^{elg D434N}::CITRINE$ T1 plants (60 of 201). Next, we selected plants in T2 that harbored similar expression level. At similar expression, $BAK1prom:bak1^{elg D434N}::CITRINE$ plants showed already a strong phenotype but $BAK1prom:bak1^{D434N}::CITRINE$ were indistinguishable from wild-type (see Fig. 4A of the main text).

Table S1. Primer list

Primer name	Sequence
UBQ10prom-B4	GGGGACAACCTTTGTATAGAAAAGTTGCTAGTCTAGCTCAACAGAGC
UBQ10prom-B1R	GGGGACTGCTTTTTGTACAAACTGCCTGTTAATCAGAAAAACT
35Sprom-B4	GGGGACAACCTTTGTATAGAAAAGTTGCTCGCGGCCAACATGGTGGA
35Sprom-B1R	GGGGACAACCTTTGTATAGAAAAGTTGCTCGCGGCCAACATGGTGGA
BRI1prom-B4	GGGGACAACCTTTGTATAGAAAAGTTGCTGATCTTCCTCTTTATTG
BRI1prom-B1R	GGGGACTGCTTTTTGTACAAACTGCTTCAAGAGTTTGTGAG
BAK1prom-B4	GGGGACAACCTTTGTATAGAAAAGTTGCTTGTTTTTGGAAACAGAG
BAK1prom-B1R	GGGGACTGCTTTTTGTACAAACTGCTTATCCTCAAGAGATTA
BRI1-B1	GGGGACAAGTTTGTACAAAAAAGCAGGCTTAACCATGAAGACTTTTCAAGCTTCTTC
BRI1noSTOP-B2	GGGGACCACCTTTGTACAAGAAAGCTGGGTATAATTTTCTTCAGGAAC
BAK1-B1	GGGGACAAGTTTGTACAAAAAAGCAGGCTTAACCATGGAACGAAGATTAATGATCCC
BAK1noSTOP-B2	GGGGACCACCTTTGTACAAGAAAGCTGGGTATCTTGGACCCGAGGGGTATT
BK11-B1	GGGGACAAGTTTGTACAAAAAAGCAGGCTTAGAAAATAATCTACAACAG
BK11noSTOP-B2	GGGGACCACCTTTGTACAAGAAAGCTGGGTATCAAGAATCCTTAACCTT
6HA-B2R	GGGGACAGCTTTCTGTACAAAGTGGCTCCTGCTGCTGCTGCTGCT
6HA-B3	GGGGACAACCTTTGTATAATAAAGTTGCTCAAGCGTAATCTGGAACGCATATGGATAGG
mCITRINE-B2R	GGGGACAGCTTTCTGTACAAAGTGGCTATGGTGAGCAAGGGCGAG
mCITRINE-B3	GGGGACAACCTTTGTATAATAAAGTTGCTTACTTGTACAGCTCGTCCATGCCG
mCHERRY-B2R	GGGGACAGCTTTCTGTACAAAGTGGCTATGGTGAGCAAGGGCGAG
mCHERRY-B3	GGGGACAACCTTTGTATAATAAAGTTGCTTACTTGTACAGCTCGTCCATGCCGCGGTGGA
BAK1-D122N-F	CTGACGGAAATTGGTGAGCTTGAATCTTTACTTGAACAATTTAAG
BAK1-D122N-R	CTTAAATTGTTCAAGTAAAGATTCAAGCTCACCAATTCGCTCAG
BAK1-D434N-F	TTGAAGCCGTGGTTGGGAATTTGGACTTGCAAAAC
BAK1-D434N-R	GTTTTGCAAGTCCAAAATCCCAACCACGGCTTCAA

Table S2. Constructs list

Construct name	Binary Vector	Resistance in plant
BAK1prom::BAK1-mCITRINE (BAK1::CITRINE)	pB7m34GW	Basta
BAK1prom::BAK1-mCHERRY (BAK1::CHERRY)	pH7m34GW	Hygromycin
BAK1prom::BAK1-6xHA (BAK1::6xHA)	pK7m34GW	Kanamycin
BAK1prom::BAK1 ^{D122N} -mCITRINE (bak1 ^{elg} ::CITRINE)	pB7m34GW	Basta
BAK1prom::BAK1 ^{D122N} -mCHERRY (bak1 ^{elg} ::CHERRY)	pH7m34GW	Hygromycin
BAK1prom::BAK1 ^{D122N} -6xHA (bak1 ^{elg} ::6xHA)	pK7m34GW	Kanamycin
BAK1prom::BAK1 ^{D434N} -mCITRINE (bak1 ^{D434N} ::CITRINE)	pB7m34GW	Basta
BAK1prom::BAK1 ^{D122N-D434N} -mCITRINE (bak1 ^{elg D434N} ::CITRINE)	pB7m34GW	Basta
BRI1prom::BRI1-mCITRINE	pB7m34GW	Basta
35Sprom::BRI1-CITRINE (OxBRI1)	pB7m34GW	Basta
UBI10prom::BK11-mCHERRY (OxBK11)	pH7m34GW	Hygromycin